The Permeability of the Endplate Channel to Organic Cations in Frog Muscle

TERRY M. DWYER, DAVID J. ADAMS, and BERTIL HILLE

From the Department of Physiology and Biophysics, SJ-40, University of Washington, Seattle, Washington 98195. Dr. Dwyer's present address is Department of Physiology and Biophysics, University of Mississippi, Jackson, Mississippi 39216.

ABSTRACT The relative permeability of endplate channels to many organic cations was determined by reversal-potential criteria. Endplate currents induced by iontophoretic "puffs" of acetylcholine were studied by a Vaseline gap, voltage clamp method in cut muscle fibers. Reversal potential changes were measured as the NaCl of the bathing medium was replaced by salts of organic cations, and permeability ratios relative to Na^+ ions were calculated from the Goldman-Hodgkin-Katz equation. 40 small monovalent organic cations had permeability ratios larger than 0.1. The most permeant including NH_4^+, hydroxylamine, hydrazine, methylamine, guanidine, and several relatives of guanidine had permeability ratios in the range 1.3–2.0. However, even cations such as imidazole, choline, tris(hydroxymethyl)aminomethane, triethylamine, and glycine methylester were appreciably permeant with permeability ratios of 0.13–0.95. Four compounds with two charged nitrogen groups were also permeant. Molecular models of the permeant ions suggest that the smallest cross-section of the open pore must be at least as large as a square, 6.5 Å × 6.5 Å. Specific chemical factors seem to be less important than access or friction in determining the ionic selectivity of the endplate channel.

INTRODUCTION

At the neuromuscular junction of vertebrate striated muscle, the natural chemical transmitter, acetylcholine, depolarizes the muscle cell membrane by opening postsynaptic ionic channels. These acetylcholine-activated channels, called endplate channels here, are selective against anions but discriminate little among small cations. Endplate channels allow Na^+ and K^+ ions to cross the membrane with nearly equal ease and tend to drive the membrane towards a potential between −15 and 0 mV when activated under physiological conditions (Fatt and Katz, 1951; Takeuchi and Takeuchi, 1960; Jenkinson and Nicholls, 1961; Takeuchi, 1963 *a*; Huang et al., 1978; Linder and Quastel, 1978). Endplate channels are large enough to be permeable to alkylammonium ions and other monovalent organic cations such as ethylammonium, Tris buffer (tris[hydroxymethyl]aminomethane), and guanidinium (Furukawa and Furukawa, 1959; Creese and England, 1970; Ritchie and Fambrough, 1975; Maeno et al., 1977; Case et al., 1977; Huang et al., 1978). In addition, they

J. GEN. PHYSIOL. © The Rockefeller University Press · 0022-1295/80/05/0469/24 $1.00 469
Volume 75 May 1980 469–492

are permeable to nonelectrolyte molecules, such as urea and ethylene glycol, and to divalent cations, such as Ca^{++}, Mg^{++}, and ethylenediamine in the doubly ionized form (Jenkinson and Nicholls, 1961; Takeuchi, 1963 *b*; Huang et al., 1978). Altogether 9 metal ions, 20 organic cations, and 5 nonelectrolyte molecules have been reported to be permeant at the endplate.

This paper and the following one (Adams et al., 1980) concern the use of ionic selectivity as a guide to the permeability mechanism of endplate channels. Our goal in the first paper is to obtain quantitative permeability measurements for a wide variety of organic cations. These observations are intended to be complete enough to permit prediction of the permeability to other, untested organic cations. More importantly, however, they can be used to define the inside dimensions of the pore in the endplate channel, on the assumption that the open pore has definite dimensions with a minimum caliber only slightly larger than the largest detectably permeant ion. Although there already are several studies of organic cation permeability (Furukawa and Furukawa, 1959; Maeno et al., 1977; Huang et al., 1978), the problem needed further investigation, inasmuch as the published conclusions were drawn from potential measurements without a voltage clamp and used many untested assumptions to be discussed later. Our results do not change the picture already developed by others, but they do add precision and scope. A preliminary report of our work has appeared (Dwyer et al., 1979).

METHODS

Dissection and Solutions

Portions of single muscle fibers, including the endplate region, were prepared from the semitendinosus muscle of *Rana pipiens* for voltage clamping by the Hille-Campbell (1976) Vaseline gap technique: a twitch fiber was pinched off and held with forceps at some distance from an endplate region and gradually pulled away from the muscle as the capillaries, connective tissue, and nerve branches were cut with fine iridectomy scissors. The criterion for suitability of the dissected piece of fiber was that a visible twitch would propagate through the endplate region when the end of the muscle fragment was stimulated with external electrodes. When 6–10 mm of fiber was freed with an undamaged endplate region, the other end was pinched off, isolating the piece to be studied. This piece was promptly transferred with forceps or sucked up in a tiny tube attached to a syringe from the standard Ringer's solution into the acrylic recording chamber containing one of two buffered isotonic "internal" solutions covering all pools and partitions. The endplate region was located, by viewing the fragment at × 200 or 500 magnification with Hoffman modulation-contrast optics (Hoffman, 1977), and positioned in the recording pool (A pool). A fine thread of Vaseline (Chesebrough-Ponds, Inc., Greenwich, Conn.) was laid across the top of the fiber at each partition, the pinched-off ends were recut in the "internal" solution, and the pools were isolated electrically by lowering the solution level to the Vaseline seals. Finally the solution in the A pool only was exchanged for the external reference solution. Fibers with short endplates were preferably selected so it was usually possible to fit the entire endplate into the 100–180 μm A pool, but some endplates extended into the Vaseline seals. About 200–500 μm of the fiber remained in each end pool after the ends were cut. The grounded pool was 250 μm wide and the Vaseline seals, 200 μm. The diameter of the fiber in the A pool averaged 130 μm. Experimental

records were taken no sooner than 30 min after the fiber ends were recut to allow sufficient time for the ions in the end-pool solutions to diffuse down the fiber axis to the endplate region. External solutions were changed by perfusing the A pool (0.15 ml of volume) with 3–5 ml of the test cation solution or 3–8 ml of external reference solution. To minimize volume changes and ion redistribution, the exposure to test solutions was limited to 90–120 s, alternated with longer periods in the reference solution. All experiments were performed at 12°C.

The external reference solution for most experiments contained 114 mM NaCl, 1 mM $CaCl_2$, and 10 mM L-histidine, pH = 7.5. In the test solutions all of the NaCl was replaced by an osmotically equivalent amount of the test salt or, in a few cases, the test salt mixed with the relatively impermeant salt D-glucosamine·HCl. For another series of experiments the external reference solution was a Ca-free, low-Na mixture: 5 mM NaCl, 109 mM glucosamine·HCl, 12 mM histidine, pH = 6.3, and the test solutions contained only 114 mM test salt and 12 mM histidine. The "internal" solution used in the main series of experiments was 115 mM NaF and 10 mM histidine, pH = 7.4, and that for the second series contained 11.5 mM NaF, 108 mM of the salt L-arginine L-aspartate, and 2 mM histidine, pH = 6.9. The osmolality of all solutions was measured to be in the range 200–225 mosmol/kg.

In choosing a buffer we needed a compound that neither blocked the response of the endplate nor contained a cation permeant at the endplate. After numerous trials we selected pure histidine base (pK_a s = 1.8, 6.0, or 9.2), which makes a solution of histidine zwitterions (no net charge) with a pH of 7.6 without further titration. Its buffer strength is weak in the range from pH 7.0 to 8.2, but becomes stronger both above and below. Because the available evidence suggests that the permeability ratio P_{Na}/P_K of endplate channels is not strongly sensitive to external pH between pH 5.2 and 9.0 (Ritchie and Fambrough, 1975; Trautmann and Zilber-Gachelin, 1976) and the myoplasm is already a good buffer, we did not attempt to bring the external or internal solutions to a specific pH. Except where noted, the measured pH of all solutions was in the range pH 6.9–7.6. However, a number of compounds studied had pK_a below 9.0. These were often studied at pH values below 7.0 to avoid having much of the neutral form in the test solution. The actual pH used and the calculated concentration of cationic form are given in the tables for these substances. The histidine buffer was normally omitted for compounds with pK_a below 7.0.

The compounds were not purified further or analyzed except for washing triaminoguanidine·HCl with ethanol. When compounds were obtained as the free amine, they were titrated with HCl to near neutrality to form the chloride salt. In the text, cations with a dissociable proton are often referred to by the simpler name of the neutral basic form. The following organic compounds were studied as test salts replacing NaCl in the test solutions: ethylamine·HCl, dimethylamine·HCl, triethylamine·HBr, di-iso-propylamine, methylethylamine·HCl, ethylenediamine, hydrazine, formamidine, *n*-butylamine, iso-butylamine, *t*-butylamine·HCl, guanidine·HCl, hydroxyguanidine·$\frac{1}{2}H_2SO_4$, aminoguanidine·HNO_3, methylguanidine·$\frac{1}{2}H_2SO_4$, guanylurea·$\frac{1}{2}H_2SO_4$, diethanolamine, 2-dimethylaminoethanol, diethylaminoethanol, 2-isopropylaminoethanol, bis(2-hydroxyethyl)dimethylammonium·Cl, triethyl(2-hydroxyethyl)ammonium·I, tetrakis(2-hydroxyethyl)ammonium·Br, tetramethylammonium·Br, tetraethylammonium·Br, choline·Cl, trimethylsulfonium·I, trimethylsulfoxonium·I (all from Eastman Organic Chemicals Div., Eastman Kodak Co., Rochester, N.Y.); imidazole, 2-aminoethanol·HCl, trimethylamine·HCl, diethylamine·HCl, triethanolamine·HCl, *n*-amylamine, benzylamine, 1,6-hexanediamine, D(+)glucosamine·HCl, tris(hydroxymethyl)aminomethane, L-histidine·HCl, L-lysine·HCl, L-arginine·HCl, 4-aminopyridine, glycine methylester·HCl, gly-

cine ethylester·HCl (all from Sigma Chemical Co., St. Louis, Mo.); acetamidine·HCl, biguanide, 1,1-dimethylbiguanide·HCl, 2-aminoethanethiol, methylhydrazine·$\frac{1}{2}H_2SO_4$, *n*-propylamine, iso-propylamine, *N*-ethyldiethanolamine, cyclohexylamine, 3,4-diaminopyridine, 4-(aminomethyl)-piperidine (all from Aldrich Chemical Co., Milwaukee, Wis.); ammonium·Cl, methylamine·HCl, hydroxylamine·HCl (all from J. T. Baker Chemical Co., Phillipsburg, N.J.); piperazine (from MC&B Manufacturing Chemists, Inc., Cincinnati, Ohio); 1,4 butanediamine (from NBC, Cleveland, Ohio); methylethyldiethanolammonium·Br (a generous gift of Dr. D. J. Triggle, State University of New York, Buffalo, N.Y.).

Recording Techniques and Equipment

The electronic arrangement for voltage clamp was similar to that of Hille and Campbell (1976) with numerous small modifications. The membrane current was measured as the voltage across a 200 kΩ resistor in the feedback loop of a current monitor. Series resistance compensation was tuned in response to a brief current step and holding current was subtracted automatically from the total membrane current with an analog circuit as follows. Early in each voltage clamp pulse, a follow-and-hold circuit was commanded to hold the value of the steady holding current at that voltage, and during the remainder of the pulse this base line was subtracted on-line from the membrane current signal to display end plate currents on a zero base line. This difference signal was then filtered with an active, eight-pole, low-pass Bessel filter at 200 Hz, displayed DC-coupled after further amplification on a dual-beam, storage oscilloscope, and photographed for later analysis. The membrane current and potential were also monitored throughout the experiment on a chart recorder.

The endplate region of the fiber, located in the A pool, was usually voltage-clamped at a holding potential of 0 mV so that the internal and external Na^+ ions would be close to equilibrium when the fiber was bathed in standard Ringer's solution and cut in NaF. A micropipette (20–30 MΩ resistance) containing 2 M acetylcholine chloride (ACh) was positioned about 20 μm from the fiber over an endplate region. Iontophoretic "puffs" of ACh were released by 10–30-ms current pulses of ~70 nA superimposed on a −4 nA braking current from an optically isolated voltage source. Approximate calculations with these conditions suggest that the ACh concentration at the endplate might reach a peak of 3 μM about 100 ms after the iontophoretic pulse. The protocol of the experiments was to step the membrane potential away from 0 mV every 12 s with 4-s voltage clamp pulses of either polarity and in multiples of 7 mV. The oscilloscope sweep and follow-and-hold circuit for the membrane current base line were triggered 2 s after the start of the step, and the iontophoretic ACh puff was delivered after another 200 ms. The endplate current rose to a peak 100–200 ms after the puff and decayed over the following second. Conditions were arranged to keep the peak currents from exceeding 10–15 nA. Since our objective was to determine the reversal potential for endplate current and not the magnitude of the endplate conductance, the position and current in the iontophoretic pipette were adjusted whenever necessary.

Determination of Reversal Potential

The reversal (zero-current) potential, E_r, for current in endplate channels was determined in the various test cation solutions from records of ACh-induced endplate currents during steps to different membrane potentials. In most experiments, the reversal potential was measured in the external reference solution, between each measurement in a test solution, in order to monitor possible changes in the condition of the fiber, and if E_r changed by as much as 3 mV, the test measurement was

rejected. The reversal potential was usually interpolated by linear regression from four values of peak current measured at 7 mV intervals straddling E_r. No value was considered unless it was based on clear inward and outward currents. Potentials were measured as inside potential minus outside, corrected for the different junction potentials between the test solutions and the 1 M KCl/agar bridge in the A pool and for the fixed junction potential in the ground and input pools. These corrected potentials are rounded off to the nearest millivolt in the labels of the figures. Junction potential measurements to the agar bridges were made with respect to a Beckmann 29402 ceramic junction, saturated KCl, reference electrode.

For solutions containing only one permeant monovalent ion, the ratio of permeabilities, P_X/P_{Na}, for the test cation X to that of sodium was calculated from changes of the reversal potential, ΔE_r, according to the equation,

$$\Delta E_r = E_{r,X} - E_{r,Na} = \frac{RT}{F} \ln \frac{P_X[X]}{P_{Na}[Na]}, \quad (1)$$

where RT/F has the value 24.66 mV at 12°C, and $[X]$ and [Na] stand for the activities of X^+ and Na^+ in the external test and reference solutions. In a few cases either the test or the control solution contained two permeant monovalent ions. If one solution contained ions X^+ and Y^+, and the other, ion Z^+, then the permeabilities were related to the reversal potential change by

$$\Delta E_r = E_{r,XY} - E_{r,Z} = 24.66 \ln \frac{P_X[X] + P_Y[Y]}{P_Z[Z]}. \quad (2)$$

The ratio P_X/P_{Na} will be referred to as "the permeability ratio for X," with Na^+ understood to be the reference ion.

These methods are derived from the Goldman-Hodgkin-Katz voltage equation (Goldman, 1943; Hodgkin and Katz, 1949). They are independent of the number of conducting endplate channels activated by ACh, but they do assume that the internal ionic concentrations and the permeability ratios are not changed by changing the external solutions. The equations make no allowance for the presumably very small contribution of anions and divalent ions to E_r. Anions are generally considered impermeant at the endplate, because changing from NaCl to sodium glutamate or other Na^+ salts has little effect on E_r (Oomura and Tomita, 1960; Takeuchi and Takeuchi, 1960; Ritchie and Fambrough, 1975) and because the ACh-stimulated ^{36}Cl fluxes in denervated diaphragm are small (Jenkinson and Nicholls, 1961). We confirm this conclusion in the following article (Adams et al., 1980). Divalent ions, on the other hand, are known to be permeant and their absence from Eqs. 1 and 2 is based on their low concentration. The inside of the muscle has a high activity of F^- ion which should keep the free divalent ion concentration below the micromolar range. The external solution contains 1 mM Ca^{++} in one series of experiments and no added divalent in the other. According to the Goldman-Hodgkin-Katz voltage equation for mixtures of monovalent and divalent ions (see, e.g., Lewis, 1979) external Ca^{++} would have the same effect as the following amount of Na^+: 4 [Ca] (P_{Ca}/P_{Na}) [1 + exp(E_r/12.33)]. Hence at negative potentials, 1 mM Ca^{++} would act like 4 × 1 × 0.3 × 1 = 1.2 mM Na^+, taking P_{Ca}/P_{Na} = 0.3 (Adams et al., 1980). This contribution is too small to affect any of our conclusions.

Reversal potential changes are given in the tables in the form: mean ± standard error of mean (number of observations). Typical errors of ±0.9 mV correspond to errors of 4% in the permeability ratios. The absolute reversal potential, E_r, for the control solution is also given to facilitate converting ΔE_r values back to absolute

reversal potentials if desired. Concentrations listed in the tables are for the cationic form of the test molecule, taking into account the pH and published pK_a if necessary, but without correcting for activity coefficients. The permeability ratios were calculated on the assumption that all monovalent cations have the same activity coefficient as the Na^+ ion.

RESULTS

Preliminary Observations

The first experiments to be described show that the endplate currents of a dissected fiber segment with ends cut in 115 mM NaF are well resolved and

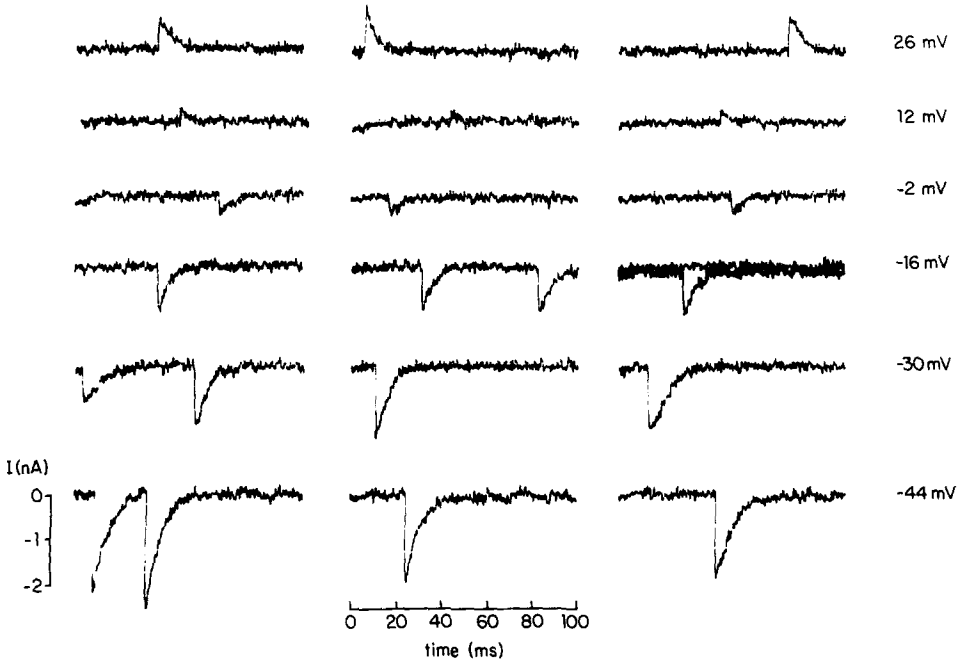

FIGURE 1. Spontaneous miniature endplate currents obtained in 114 mM NaCl, 1 mM $CaCl_2$, and 10 mM histidine using the Vaseline gap voltage clamp technique. The currents were recorded at holding potentials ranging in 14-mV steps from −44 mV to +26 mV and exhibited a reversal potential at +5 mV. Internal solution: 115 NaF. Recording bandwidth: DC to 1.8 kHz. Temperature: 12°C.

suitable for electrophysiological study. Although the presynaptic nerve fiber was cut as close as possible to the endplate, some preparations continued to produce spontaneous miniature endplate currents (MEPCs) for half an hour. Fig. 1 shows spontaneous MEPCs under voltage clamp conditions; the current signal was filtered with a high-frequency cutoff (−3 dB) of 1.8 kHz. The holding potential was changed in 14-mV intervals from −44 mV to +26 mV. At any one holding potential successive quantal currents were similar but not identical in time-course and amplitude. Most MEPCs rose to a sharp peak

rapidly, and a few had more rounded tops. For the currents in Fig. 1, the reversal potential E_r was +5 mV, and at −44 mV the peak chord conductance was 45 nS and the time constant of decay, 6 ms (12°C). The peak conductance and decay time are within the range reported for MEPCs of intact fibers and the reversal potential E_r is several millivolts more positive (see later). The records also show that base-line drift and noise in this DC-coupled system are low enough to resolve 250-pA MEPCs (e.g., at +12 mV) with a 1.8 kHz frequency response.

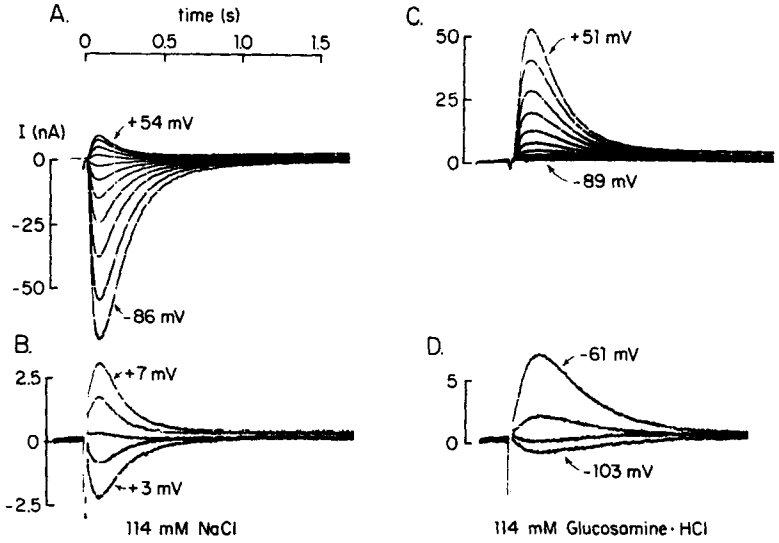

FIGURE 2. ACh-induced endplate currents obtained in the Na^+ reference solution and in a Na^+-free solution containing glucosamine·HCl and 1 mM $CaCl_2$. Membrane potentials were stepped from 0 mV 200 ms before the start of the sweep, and brief puffs of ACh were released from an iontophoretic electrode at the negative going artifact in each record. (A) Endplate currents with external 114 mM NaCl during step polarizations ranging from −86 mV to + 54 mV in 14-mV intervals. (B) Currents recorded in the same solution but at higher gain and at membrane potentials in the narrow range between +3 mV and +7 mV to show the reversal potential more clearly. (C) Endplate currents obtained on replacing NaCl entirely by the less permeant cation, glucosamine·HCl. Step polarizations ranging from −89 mV to +51 mV in 14-mV steps. (D) Currents in the glucosamine solution at higher gain and potentials between −103 mV and −61 mV. (A), (B), and (C) are from the same fiber. Internal solution: 115 NaF. Recording bandwidth: DC to 200 Hz.

All subsequent experiments in this paper deal with endplate currents induced by iontophoretic puffs of ACh and recorded with a high-frequency cutoff of 200 Hz. The superimposed current traces in Fig. 2 A are recorded during voltage steps ranging from −86 to +54 mV in intervals of 14 mV. Both the beginning and the end of the voltage steps occur outside the picture, and the time of each 1.4-nC iontophoretic puff from the ACh pipette is given

by a brief downward artifact preceding each major deflection. The induced endplate currents last about 200 ms at +54 mV, and about three times longer at −86 mV. A wide separation of the traces at negative potentials and their crowding together at positive potentials indicates that the peak current-voltage relation is quite nonlinear, with a high slope conductance for inward current and a low slope conductance for outward current. Fig. 2 B shows induced endplate currents at higher resolution near the reversal potential, with voltage steps ranging from +3 to +7 mV in 1 mV intervals. The peak conductance is about 1 μS, and the currents show an unambiguous reversal around +5 mV. For 83 fibers the mean (±SE) reversal potential was 1.8 ± 0.6 mV with 114 mM NaCl, 1 mM $CaCl_2$, and 10 mM histidine in the external solution and 115 mM NaF and 10 mM histidine in the end pools. The reversal potential for currents induced by iontophoretic puffs of ACh always coincided with the reversal potential for spontaneous MEPCs. If the endplate channel acted as a pure Na^+ electrode and if the myoplasm reached equilibrium with the 115 mM NaF solutions at the cut ends, then the expected reversal potential would be +0.2 mV, taking into account published activity coefficients. The 1.6 mV difference between prediction and observation must represent deviations from these assumptions and residual errors in our method.

Relative permeability measurements can be made with confidence only if a fairly impermeant ion is available, to show by a large change in reversal potential that the solution changes are adequate and that the permeant ions in the control solution have been identified. When the NaCl in our external control solution was entirely substituted by glucosamine·HCl, the inward endplate currents at moderately negative voltages were replaced by outward currents (Fig. 2 C) as would be expected if an external permeant ion were substituted by an impermeant one. The current-voltage relation was also changed to have a very shallow slope for hyperpolarizations and a steep slope for depolarizations. In addition, at positive potentials, e.g., +51 mV, the ACh-induced conductance change lasted twice as long as before. Higher gain records combined with a stronger iontophoretic puff of ACh revealed transient outward currents at −61 and −75 mV and small but definite inward currents at −89 and −103 mV (Fig. 2 D). With the removal of Na^+ ions, the reversal potential E_r for endplate currents therefore changed by at least −80 mV. According to Eq. 1, a ΔE_r of −80 mV is equivalent to a permeability ratio for a monovalent ion of 0.04. However, from this experiment alone it is not possible to say if $P_{\text{glucosamine}}/P_{\text{Na}}$ actually is 0.04, as glucosamine could be even less permeant and some of the inward current might be due to the 1 mM Ca^{++} ion or the few millimolar ionized histidine molecules in the solution or to contamination by an impurity, by Na^+ leaking from the fiber or through the seals from the side pools, or by Na^+ remaining from an imperfect solution change. More complete measurements of the permeability of glucosamine, histidine, and Ca^{++} cations are given later in this paper and in the next paper (Adams et al., 1980). For the moment, this experiment suggests that the relative permeabilities of pure test compounds with permeability ratios significantly larger than 0.04 can be studied in our system without further precaution.

In studies of permeability and selectivity, both the current amplitudes and reversal potentials are of theoretical interest. The endplate currents in Fig. 3 show that these two quantities change when the cation in the test solution is changed. The measured reversal potentials are +7 mV for 114 mM sodium, +13 mV for 114 mM methylamine, and +20 mV for 114 mM guanidine, making the sequence of permeability ratios sodium < methylamine < guanidine. On the other hand, the sequence of current sizes is guanidine < sodium < methylamine. Such a disparity is not surprising in that many cations are known to have "pharmacological effects" which would affect the number of channels opening in iontophoretic experiments. Indeed, in our experience with over 60 test ions, there was little correlation between the conductance and the permeability ratios calculated from reversal potentials. With some cations that were obviously of the right size to be permeant, e.g., tetramethylammo-

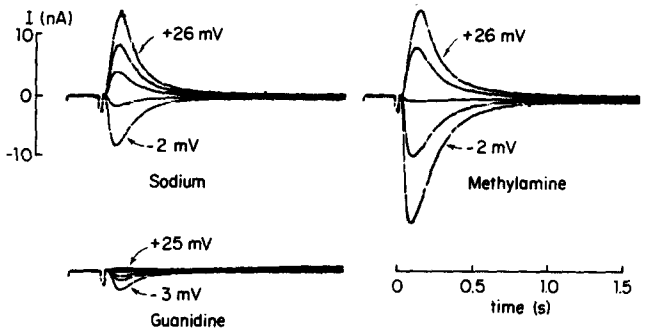

FIGURE 3. Endplate currents induced by brief iontophoretic puffs of ACh in solutions with highly permeant cations. External medium contains 114 mM Na^+, methylamine, or guanidine. The pulse delivered to the iontophoretic electrode and the gain of the current trace is the same in the three panels. Both reversal potential and peak endplate conductance depend on the permeant ion. Potentials at 7-mV intervals. Internal solution: 115 mM NaF. Temperature: 12°C.

nium, the pharmacological effects were so strong that no endplate currents could be detected. Hence in this paper we use only the reversal potentials as an index for permeability ratios. A later section summarizes some of the apparent pharmacological effects on current amplitudes and time-courses.

Endplate Channels are Permeable to Many Organic Cations

We have found 40 clearly permeant, monovalent organic cations as judged by their ability to carry net inward current in endplate channels with a reversal potential equivalent to permeability ratios in the range 0.1–2.0.

In the first series of selectivity studies, each test cation was studied on a minimum of six different fibers with ends cut in 115 mM NaF and 10 mM histidine. The permeability to methylammonium and guanidinium cations has been documented by the inward currents shown in Fig. 3. For the actual

selectivity measurements, the gain of the current trace was increased and voltage steps were restricted to a few levels at 7-mV intervals near the reversal potential, as in the traces of Fig. 4. These records show current reversals and inward currents with solutions of dimethylammonium, diethanolammonium, Tris (at pH = 6.8), biguanide, and imidazole (at pH = 6.0) salts. Changes of reversal potential, ΔE_r, relative to the 114 mM Na^+ reference solution were measured from records like those of Fig. 4, and permeability ratios P_X/P_{Na} were calculated with Eq. 1.

Table I summarizes the mean ΔE_r and calculated permeability ratios for solutions of 28 different ammonium cations which are saturated combinations of alkyl, amino, hydroxyl, and sulfhydryl groups added to the ammonium nucleus. Five of the simplest ammonium ions are more permeant than Na^+

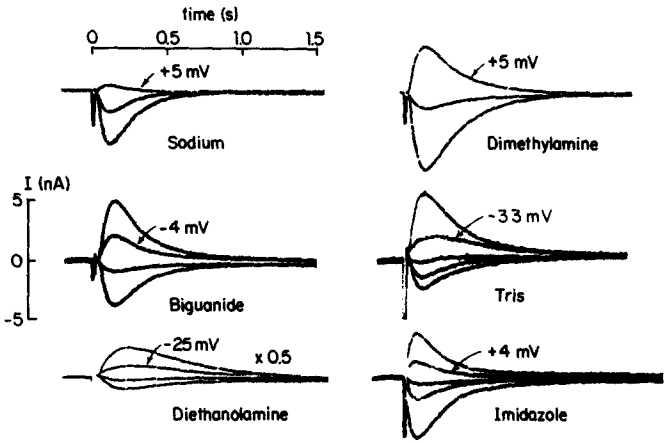

FIGURE 4. Reversal potential measurements with five permeant organic cations substituting for sodium. Current records with potential steps at 7-mV intervals for solutions containing approximately 114 mM sodium, dimethylamine, biguanide, Tris (pH 6.8), diethanolamine, and imidazole (pH 6.0). Traces in diethanolamine were recorded at a lower gain (× 0.5). Internal solution: 115 NaF. Temperature: 12°C.

ions. They are ammonium itself and its hydroxyl, amino, methyl, and ethyl derivatives. The reversal potentials for solutions of a few of the larger compounds near the bottom of Table I are so negative that they may be limited by incomplete solution changes and leak of Na^+ ions through the seals from the side pools. These measurements, placed in parentheses, are not so reliable as another series discussed later and designed for compounds of low permeability. Table I also gives the molecular weight and the number of major atoms (the nonhydrogen atoms) in each cation. For saturated compounds containing only C, N, O, and H, both weight and number of major atoms give an indication of molecular volume, and as a rough rule, the observations suggest that the relative permeability at the endplate decreases with increasing size of the organic test ion. This inverse relationship is seen in the plot of permeability

ratio vs. molecular weight in Fig. 5 A. The circles represent all the permeability ratios from Table I, except (triangles) those where better values were available from other experiments given later. Cations with molecular weights below 47 and with three or fewer major atoms have measured permeabilities from 0.87 to 1.92 that for Na^+, and cations with molecular weights above 110 and with eight or more atoms have permeabilities less than 0.2 that for Na^+. A smooth curve has been drawn to suggest the trend. The most prominent outlying point is that for sulfur-containing 2-aminoethanethiol with a permeability ratio of 0.94 and molecular weight of 78.2.

TABLE I

ΔE_r AND PERMEABILITY RATIOS FOR SATURATED ORGANIC CATIONS

$\Delta E_r \pm$ SE		Concn (X)	Mol wt	Major atoms	P_x/P_{Na}	X
mV	*n*	*mM*				
12.4±0.5	(6)	98	34.0	2	1.92	Hydroxylamine (pH = 5.1)
14.3±0.9	(8)	114	18.5	1	1.79	Ammonium
7.2±0.6	(10)	114	32.1	2	1.34	Methylamine
5.9±0.6	(6)	110	33.1	2	1.32	Hydrazine (pH = 6.6)
2.9±0.4	(6)	114	46.1	3	1.13	Ethylamine
−1.6±0.6	(7)	114	78.2	4	0.94	Aminoethanthiol
−3.4±0.1	(7)	114	46.1	3	0.87	Dimethylamine
−4.8±0.6	(7)	114	60.1	4	0.82	Isopropylamine
−6.6±0.8	(7)	114	60.1	4	0.77	Methylethylamine
−8.0±0.2	(8)	114	62.1	4	0.72	Ethanolamine
−9.4±0.4	(7)	114	60.1	4	0.68	*n*-Propylamine
−13.2±0.2	(8)	100	61.1	4	0.68	Ethylenediamine (pH = 8.4)
−20.3±0.5	(6)	114	76.1	5	0.44	Methylethanolamine
−20.9±0.6	(7)	114	74.2	5	0.43	*n*-Butylamine
−23.6±0.5	(9)	114	74.2	5	0.38	Diethylamine
−27.0±1.2	(8)	114	60.1	4	0.36	Trimethylamine
−29.9±1.2	(6)	114	77.2	4	0.30	Trimethylsulfonium
−31.2±0.8	(6)	109	87.1	6	0.30	Piperazine (pH = 7.0)
−30.5±0.7	(6)	114	74.2	5	0.29	Isobutylamine
−33.8±0.7	(10)	114	106.2	7	0.25	Diethanolamine
−36.5±1.0	(6)	114	90.1	6	0.23	Dimethylethanolamine
−43.2±0.4	(6)	108	122.1	8	0.18	Tris (pH = 6.8)
−43.2±0.7	(6)	114	104.2	7	0.17	Isopropylethanolamine
−46.9±2.7	(6)	114	118.2	8	0.15	Diethylethanolamine
(−72.4±1.2)	(7)	20	104.2	7	<0.15*	Choline
(−58.7±1.3)	(7)	114	150.2	10	<0.09	Triethanolamine (pH = 6.6)
(−67.0±0.6)	(6)	114	134.2	9	<0.07	Dimethyldiethanolammonium
(−78.8±1.6)	(10)	109	180.2	12	<0.043	Glucosamine (pH = 6.3)

Reference solution: 114 mM NaCl, 1 mM $CaCl_2$, 10 mM histidine. End-pool solution: 115 mM NaF, 10 mM histidine. E_r = 1.8 ± 0.6 mV in reference solution.

* Calculation takes into account 94 mM glucosamine with permeability ratio 0.033.

Table II lists measured reversal potential changes and the calculated permeability ratios for 15 other cations containing C=N, C=O, and S=O double bonds. Five of these unsaturated cations are more permeant by this criterion than Na^+. These are guanidine, hydroxy- and aminoguanidine,

acetamidine, and formamidine, all planar compounds with resonating N—C—N bond systems. As with the saturated compounds, the largest unsaturated cations tend to be the least permeant, e.g., lysine and arginine are near the 1% level, and the smaller cations are the more permeant. However, a plot of permeability ratio against molecular weight (Fig. 5 B) shows more scatter and a tendency towards higher permeability at each molecular weight than was found for saturated cations (smooth line copied from Fig. 5 A).

Large Cations Have Very Low Permeability Ratios

In the experiments of Tables I and II, six of the solutions gave very negative reversal potentials ranging from −58 to −84 mV. Since a −58 mV reversal potential can be produced by a solution containing but 8 mM Na^+ ions

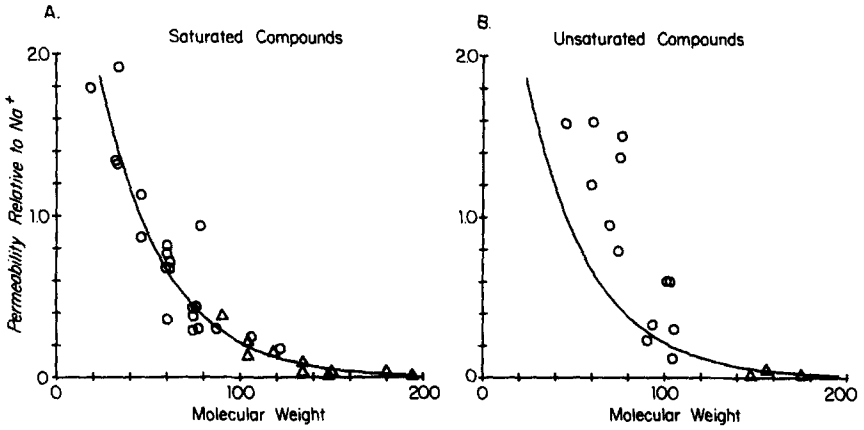

FIGURE 5. Relationship between relative permeability (P_X/P_{Na}) at the endplate and molecular weight for all monovalent organic cations studied. (A) Saturated organic cations. (B) Unsaturated organic cations. The ends of the muscle fibers were cut in either 115 NaF (○) or in 11 mM NaF plus 108 mM arginine aspartate (△). The smooth curves are the function, 3.6 exp(−0.028· mol wt), drawn to suggest the trend.

(Adams et al., 1980), some precautions needed to be taken with cations of low permeability that contamination by Na^+ and by other permeant cations was not the cause of the inward current. Some potential sources of unwanted permeant ions are (*a*) the histidine and 1 mM Ca^{++} in the external solution, (*b*) remaining Na^+ ion from the washes with reference solution between each test, and (*c*) Na^+ ion leaking from the fiber and through the grease seal around the fiber from the 115 mM NaF solution in the side pools. Each of these sources of contamination was reduced or shown to be unimportant in a second series of selectivity measurements designed to measure reversal potentials with compounds of low permeability. The three major improvements in this second experimental series were to eliminate Ca^{++} ion from all solutions, to lower the Na^+ content of the end pool solutions to 11.5 mM, and to lower

the Na^+ content of the external reference solution used between each test to 5 mM (see Methods). Finally, the permeability to histidine cations was shown to be too small to affect the measurements (see next paragraph). Cutting the fibers in 11.5 mM Na^+ instead of 114 mM Na^+ made the absolute reversal potentials an average of 45 mV more positive in comparable solutions including low-Na Ringer's, showing that the internal Na^+ activity had fallen approximately sixfold to 18 mM. The absolute reversal potential in the Ca-free, 5 mM Na^+-reference solution was -24.1 ± 1.2 mV ($n = 36$). Changes of reversal potential, ΔE_r, were measured with respect to this value.

To our surprise, several ions such as choline, triethylamine, *t*-butylamine, and 4-aminopyridine which depressed inward and outward endplate currents

TABLE II

ΔE_r AND PERMEABILITY RATIOS FOR UNSATURATED ORGANIC CATIONS

$\Delta E_r \pm$ SE		Concn (X)	Mol wt	Major atoms	P_x/P_{Na}	X
mV	*n*	*mM*				
Guanidinium and amidinium cations						
11.4±1.1	(7)	114	60.1	4	1.59	Guanidine
11.3±0.4	(6)	114	45.1	3	1.58	Formamidine
−31.2±0.9	(6)	19	76.1	5	1.50*	Hydroxyguanidine
7.8±0.9	(7)	114	75.1	5	1.37	Aminoguanidine
4.5±0.2	(7)	114	59.1	4	1.20	Acetamidine
4.3±0.5	(8)	171	74.2	5	0.79	Methylguanidine
−34.4±1.0	(9)	43	102.1	7	0.60*	Guanylurea
−12.6±0.6	(6)	114	102.1	7	0.60	Biguanide
−29.6±0.1	(6)	114	105.2	7	0.30	Triaminoguanidine
Other cations						
−4.3±0.5	(6)	101	69.1	5	0.95	Imidazole (pH = 6.0)
−27.6±0.8	(6)	114	93.2	5	0.33	Trimethylsulfoxonium
−36.6±0.8	(6)	114	90.1	6	0.23	Glycine methylester (pH = 5.9)
−51.7±0.9	(5)	114	104.1	7	0.12	Glycine ethylester (pH = 5.7)
(−82.5±2.0)	(6)	114	147.2	10	<0.035	Lysine
(−80.4±2.0)	(6)	114	175.2	12	<0.038	Arginine

All conditions identical to Table I.

* Calculations take into account the glucosamine in these solutions.

strongly (see later section) in fibers cut in 115 mM Na, gave large, clear currents in fibers cut in low-sodium solutions. Fig. 6 shows endplate currents with solutions containing 5 mM Na (the external reference solution), 114 mM choline, 114 mM glucosamine, 160 mM histidine (only half ionized at pH 6.0), 114 mM triethylamine, 114 mM 4-aminopyridine, and 114 mM *t*-butylamine. The reversal potential changes, ΔE_r, obtained under these conditions for 16 poorly permeant cations are listed in Table III. With the improved method, reversal potentials for arginine, lysine, tetrakisethanolammonium, and methylethyldiethanolammonium solutions are 20–30 mV more negative than that for glucosamine, suggesting that glucosamine is not an absolutely impermeant sodium substitute. This result complicates the quan-

titative interpretation of the observations, as the 5 mM Na^+ external reference solution for all ΔE_r measurements also contained 110 mM glucosamine. Therefore, Eq. 2 for mixtures of two permeant ions has to be used in analyzing the ΔE_r on changing from the control solution to the test solutions. From the -20.0 ± 1.5 mV ΔE_r obtained when switching from reference solution to glucosamine test solution, one can calculate a permeability ratio of 0.034 ± 0.002 for glucosamine. This value was assumed in calculating all the other permeability ratios in Table III, and elsewhere in these papers we use a permeability ratio of 0.033. In effect, the 110 mM glucosamine of the reference

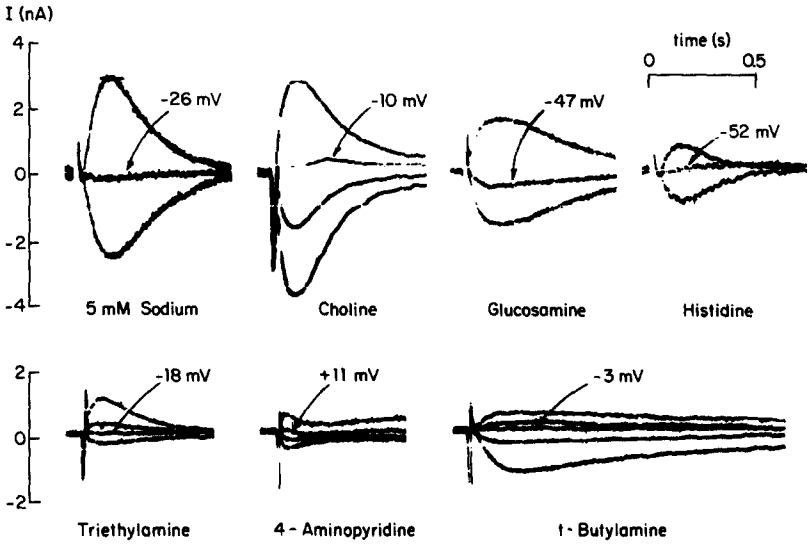

FIGURE 6. ACh-induced endplate currents obtained with Ca-free external solutions containing 5 mM sodium or a poorly permeant organic cation. Current records were measured at the following step potentials: 5 mM Na + 108 mM glucosamine (−31, −26, −19 mV); 114 mM choline (−24, −17, −10, −3 mV); 114 mM glucosamine (−61, −47, −33 mV); 160 mM histidine (−66, −45, −38 mV); 114 mM triethylamine (−32, −18, −4, +17 mV); 114 mM 4-aminopyridine (−17, −3, +11, +25 mV) 114 mM *t*-butylamine (−31, −17, −3, +11, +25 mV). All records were obtained with fiber ends cut in a low-sodium solution: 11.5 mM NaF, 108 mM arginine aspartate, 2 mM histidine. Temperature: 12°C.

solution acts like an additional 3.7 mM Na^+. The 10 mM histidine buffer in all solutions adds an additional quantity of permeant ions. With a pK_a of 6.0, no more than half the histidine would ever be ionized in our solutions. Table III shows that histidine cations have a permeability ratio of 0.043, so the maximum of 5 mM histidine cations should act like no more than 0.2 mM Na^+ ions.

The measurements of Table III show that electrical techniques can achieve a high sensitivity in our preparation after some precautions are taken. Four ions have permeability ratios around the 0.01 level. Why did lysine and

arginine seem less permeant in the measurements in Table II than in those of Table III? Possible artifacts from Ca^{++} ions, histidine cations, or chemical impurities can be ruled out on quantitative grounds, leaving contamination from extracellular Na^+ ions as the remaining explanation. The Na^+ ions might persist from the control solution, leak from the fiber, or, perhaps most plausibly, enter the test pool from the end pool via the collar of extracellular space in the seal around the fiber, all defects that could have been reduced by using continuously flowing test solutions. The same problem exists to a smaller extent for the measurements of Table III. For this reason, four measurements with an absolute reversal potential more negative than −60 mV ($\Delta E_r < -36$ mV) have been placed in parentheses and the calculated permeability ratios

TABLE III

ΔE_r AND RELATIVE PERMEABILITY FOR POORLY PERMEANT ORGANIC CATIONS

$\Delta E_r \pm$ SE		Concn (X)	Mol wt	Major atoms	P_x/P_{Na}	X
mV	*n*	*mM*				
+48.4±1.1	(7)	114	95.1	7	0.54	4-Aminopyridine
+39.4±0.9	(6)	114	90.1	6	0.38	Dimethylethanolamine
+31.8±1.0	(6)	114	74.2	5	0.28	*t*-Butylamine
+26.5±0.5	(6)	114	104.2	7	0.22	Isopropylethanolamine
+15.9±1.4	(6)	114	118.2	8	0.15	Diethylethanolamine
+13.8±1.3	(7)	114	104.2	7	0.13	Choline
+4.2±1.6	(6)	112	134.2	9	0.090	Dimethyldiethanolammonium
+4.1±0.5	(6)	114	102.2	7	0.090	Triethylamine
−22.9±1.2	(6)	80	156.2	11	0.043	Histidine (pH = 6.0)
−20.0±1.5	(7)	109	180.2	12	0.034	Glucosamine (pH = 6.3)
−21.6±1.2	(7)	112	134.2	9	0.030	Ethyldiethanolamine (pH = 6.6)
−23.4±1.8	(6)	112	150.2	10	0.030	Triethanolamine (pH = 6.6)
(−41.2±1.3)	(6)	114	175.2	12	<0.014	Arginine
(−49.2±6.5)	(5)	114	194.3	13	<0.010	Tetrakisethanolammonium
(−50.8±1.8)	(6)	114	147.2	10	<0.010	Lysine
(−53.4±2.1)	(6)	112	148.2	10	<0.009	Methylethyldiethanolammonium

Reference solution: 5 mM NaCl, 0 mM $CaCl_2$, 110 mM glucosamine HCl, 10 mM histidine. End-pool solutions: 11.5 mM NaF, 108 mM arginine aspartate, 2 mM histidine. E_r = −24.1 ± 1.4 mV (36) in reference solution.

are given as upper limits. Without further chemical analysis we could also not rule out the possibility of contamination. For example, if the 115 mM arginine solution contained 0.6 mM NH_4^+ or other small amine, the observed inward current could be entirely due to the contaminant. Having made this caveat, we accept the results at face value in the remainder of the paper. The permeability ratios in Table III are shown as triangles in Fig. 5 A and B.

Some Divalent Cations Are Permeant

Four organic compounds had two amino groups that both could be protonated in the pH range accessible to study. Reversal potentials were measured with these diamines at a pH low enough for 97% of the molecules to be doubly

charged. Three were studied on fibers cut in 115 mM NaF. These gave the following absolute reversal potentials with 80 mM of the dihydrochloride outside: 1,2-ethanediamine (pH = 6.0) −9.0 ± 0.6 mM (n = 8); 1,4-butanediamine (pH = 6.85) −8.6 ± 0.4 mV (n = 6); and 1,6-hexanediamine (pH = 5.9) −14.7 ± 0.7 mV (n = 6). One compound, 4-aminomethylpiperidine, was studied at 80 mM (pH = 6.9) on fibers cut in 11.5 mM NaF. The absolute reversal potential was +8.5 ± 0.8 mV (n = 7). All of these reversal potentials are more positive than those found with 80 mM $CaCl_2$ or other divalent alkaline earth and transition metal ions (Adams et al., 1980). Calculations with the standard Goldman-Hodgkin-Katz formalism (Eq. 1 in the following article, Adams et al., 1980) give permeability ratios with respect to Na^+ ions of 0.4 for ethane- and butanediamine, 0.3 for hexanediamine, and 0.2 for 4-aminomethylpiperidine. The permeability ratios with respect to Ca^{++} ions (at 80 mM) are 1.2–2.7.

Ion Effects on Endplate Current Amplitude and Time-Course

Many reproducible changes of the time-course and amplitude of endplate currents were seen in our experiments. Well-known factors affecting peak conductance or time-course include distance to iontophoretic pipette, solution viscosity, rate constants for opening and closing of channels, block of receptors or channels, desensitization, activity of the esterase, conductance of single open channel, etc. Each of these factors has been reported to depend on the ions in the bathing medium. The changes observed in our experiments are given but cannot be related to specific contributing factors because of the simple experimental protocol used. A study of single-channel currents and lifetimes would help considerably in clarifying these questions.

The changes of endplate current amplitude or conductance are listed here in order of decreasing size of current. Most of the changes are not evident in the figures of this paper because the position of the iontophoretic pipette and the current delivered were usually adjusted to compensate for them. (*a*) Simple, highly permeant ammonium derivatives always increased the endplate conductance: ammonium, methyl-, dimethyl-, and ethylamine, and hydrazine. (*b*) Some compounds gave "use-dependent block" in fibers cut in 115 mM NaF and, where tested, little block in fibers cut in 11.5 mM NaF (with use dependence, each ACh puff elicited less current than the preceding one at 0.1 Hz): all seven ethanolamine derivatives, including choline but not ethanolamine itself; guanidine (see Fig. 3) and its seven derivatives (c.f., Farley et al., 1979); di-ethyl-, *n*- and iso-propyl-, and *n*- and iso-butylamine; trimethylsulfonium and -sulfoxonium; and the two glycine esters. (*c*) Some compounds blocked inward and outward currents completely in fibers cut in 115 mM NaF and blocked in a use-dependent manner in fibers cut in 11.5 mM NaF: *t*-butyl- and triethylamine, tetrakisethanolammonium, and 4-aminopyridine. (*d*) There were no endplate currents with some compounds in any fibers: cyclohexylamine, di-isopropylamine, and 3,4-diaminopyridine. (*e*) Two hydrophobic compounds were toxic and eliminated endplate currents irreversibly: *n*-pentylamine and benzylamine.

The most common change of time-course of the endplate currents was a

lengthening of the time to peak and a slowing of the decay. An example with glucosamine is shown in Fig. 2 and another with t-butylamine, in Fig. 6. This effect was seen with trimethyl-, triethyl-, diethanol-, triethanol-, and *t*-butylamine, trimethylsulfonium and sulfoxonium, and glucosamine. For many of these compounds the slowing was not quickly reversed by washing with control solution. A different effect on the time-course led to some ambiguity in the determination of E_r, for at voltages very close to E_r the current might be inward for $\simeq$100 ms and then become outward for the remainder of the time. Such biphasic currents were seen in experiments with each of the hydroxyl-containing ions diethanol-, dimethylethanol-, dimethyldiethanol-, and hydroxylamine as well as with histidine. Biphasic currents might suggest an artifact from some kind of nonuniformity, but we did not identify the source, and the effect was reproducible with the appropriate solutions in fibers that with other solutions gave normal endplate currents. Where such currents occurred, only one of the 7-mV voltage levels gave actually biphasic currents, and the early part of the record was ignored in the analysis.

The four divalent, organic cations reduced the peak current amplitude, without use dependence, and also speeded the decay of each response appreciably.

DISCUSSION

Comparison with Previous Work

We have reported reversal potentials measured with 52 different monovalent organic cations and 4 divalent organic cations. The permeability sequence is inversely correlated with the size of the cation. The endplate conductance is not well correlated with permeabilities calculated from reversal potentials. Insofar as related observations have already been made by others, there is substantial qualitative agreement with their conclusions. However, few organic permeability sequences have been determined by the reversal potential criterion before, so no close comparisons can be made.

Fatt (1950) found that isotonic choline chloride by itself will depolarize at the endplate. In their pioneering study Furukawa and Furukawa (1959) observed large endplate potentials when some of the external sodium was replaced by NH_4^+, methyl-, or ethylamine. Dimethyl- and isopropylamine also supported endplate potentials, but less well. Koketsu and Nishi (1959) found that hydrazine cations restore neuromuscular transmission to preparations blocked by immersion in isotonic sucrose. Maeno et al. (1977) reported voltage measurements with 12 organic cations made by the moving electrode method in whole muscles bathed in 0.1–1.0 mM ACh. They noted the inverse relationship between permeability and size. For cations which we find to have permeability ratios larger than 0.1, Maeno et al. (1977) estimated permeability values averaging 50% of ours; for less permeant cations, they reported values consistently higher than ours. Nevertheless, considering the many assumptions of the moving electrode method, the agreement is remarkable. Ritchie and Fambrough (1975) concluded that Tris ions are permeant in rat myotube cholinergic channels since the reversal potentials of ACh responses were more

positive in sodium Tris mixtures than in sodium sucrose mixtures. Linder and Quastel (1978) estimated that NH_4^+ may be 10% more permeant than Na^+ in mouse diaphragm on the basis of a more positive reversal potential and a larger conductance change for miniature endplate potentials. Lassignal and Martin (1977) measured reversal potentials of ACh responses in the cholinergic synapse of electric eel electric organs. Using mixtures of Na^+, K^+, Ca^{++}, and glucosamine (not pure solutions), they estimated a permeability ratio of 0.2 for glucosamine.

Other studies have been done by tracer methods. Creese and colleagues (Creese and England, 1970; Case et al., 1977) showed that ^{14}C-labeled decamethonium and carbachol enter rat diaphragm muscles through open endplate channels. The apparent permeability for Na^+ and decamethonium (at 10 μM) were similar, neglecting the different effects of membrane potential on a monovalent and a divalent ion. Huang et al. (1978) determined selectivity in K^+-depolarized chicken myotubes by comparing ACh-stimulated influxes of ^{22}Na with influxes of ^{14}C-labeled charged and uncharged organic molecules. The permeability ratios given for six monovalent organic cations averaged 73% of ours. For the singly charged and doubly charged forms of ethylenediamine, they found values of 0.63 and 0.57, while our values are 0.68 and 0.43. For Tris they gave 0.11, while we find 0.18. Although flux and reversal potential measurements are not expected to agree in general, there seems to be good agreement in this case probably because the flux measurements are done at a constant potential (near 0 mV) with low (1–10 mM) concentrations of the test molecule. Huang et al. (1978) also gave permeability ratios of 0.12–0.19 for the nonelectrolytes, urea, formamide, and ethylene glycol, and 0.04–0.05 for thiourea and glycerol.

Factors Influencing Permeability Ratios

CHEMICAL FACTORS The major determinant of permeability in endplate channels seems to be the size of the ion, a theme we return to shortly. In addition, within a group of ions with a similar number of atoms there may be some chemical influences on permeability. Unfortunately none of the chemical generalizations rests on a broad base of evidence, and each would require study of additional series of relevant cations to become more convincing. For example, the advantage of a linear rather than a branched-chain structure may be reflected in the sequences (permeability ratios): *n*-butylamine (0.43) > *t*-butylamine (0.28); methylethylamine (0.77) > trimethylamine (0.36); and diethanolamine (0.25) > triethylamine (0.09). The advantage of double bonds or planarity may be reflected in the sequence, aminoguanidine (1.37) > isobutylamine (0.29), and in the general observation made in Fig. 5 B that most unsaturated compounds are more permeant than saturated ones of the same molecular weight. Huang et al. (1978) said that hydrogen bonding promoted permeability, while Maeno et al. (1977) said it was not important. Indeed, several examples suggesting an advantage of hydrogen bonding can be found, but the idea is not consistently borne out, as in the similar permeabilities of the pairs: hydrazine (1.32) ≃ methylamine (1.34) and ethanolamine (0.72) ≃ methylethylamine (0.77). Finally, even charge does not

play the determining role that it has in some other channels. The endplate channel has a similar apparent permeability to neutral formamide or glycerol as it does to monovalent *n*-butylamine, diethanolamine or Tris, and to divalent ethylenediamine or 1,4-butanediamine (or even Ca^{++}). On the other hand, so far as is known anions are not permeant (Oomura and Tomita, 1960; Takeuchi and Takeuchi, 1960; Jenkinson and Nicholls, 1961; Takeuchi, 1963 *a*; Ritchie and Fambrough, 1975, Adams et al., 1980). Three of the test molecules we studied had one negative charge and two positive charges. These compounds, histidine, lysine, and arginine, had very low permeability ratios of 0.043, <0.010, and <0.009. Perhaps the presence of a negatively charged group helps to lower their permeability, but these molecules are also relatively large.

SIZE Fig. 5 showed the correlation between size, as measured by molecular weight, and permeability. In order to study this question further, we constructed Corey-Pauling-Koltum (CPK) space-filling molecular models of all the cations, measured their dimensions, and tested them for fit into holes of various sizes. The dimensions were defined as the size of a rectangular box that would hold the model, a somewhat loose concept as most cations could be placed in a wide variety of conformations differing somewhat in dimensions. The models were built with hydrogen-bonding hydrogens at all appropriate positions to represent their size as seen by a channel lined with oxygens. Consider glucosamine, ethyldiethanolamine, and triethanolamine, the largest measurably permeant ions with measured relative permeabilities of 0.034, 0.030, and 0.030 (Table III). If the pore were a long circular cylinder, it would have to be a diameter of 7.4, 7.2, or 7.1 Å to accommodate these ions. Triaminoguanidine with a relative permeability of 0.30 would need a cylindrical pore of diameter 6.6 Å. Methylethyldiethanolammonium and tetrakisethanolammonium with permeability ratios of <0.01 would require cylindrical pores of diameter 7.2 and 8.0 Å.

The same compounds can be accommodated in pores of smaller cross-sectional area if the pore were square rather than circular. The broadest parts of the molecule could then extend the width of the diagonal. We suggest the square pore with cutoff corners shown in Fig. 7 as a realistic model of the narrowest part of the endplate channel. The pore is 6.5 × 6.5 Å with 0.5 $Å^2$ cut off at each corner, making the diagonal 7.7 Å and the area 40.3 $Å^2$. A physical model made to these dimensions passes all the ions listed in Tables I–III with the exception of tetrakisethanolammonium, and could not be made much smaller and still pass such clearly permeant ions as choline, diethylethanolamine, Tris, and triaminoguanidine. On geometric grounds, at least, such a pore could be permeable to many larger molecules capable of assuming an elongated, spindle shape such as arginine, lysine, ACh, carbachol, nicotine, hexamethonium, decamethonium, succinylcholine, epinephrine, atropine, benzocaine, and procaine (but not lidocaine). It would just barely pass methyltriethylammonium and exclude tetraethylammonium. The postulated pore is large enough for about 4.5 water molecules to occupy any cross section, and therefore the open endplate channel would contain a continuous column of water molecules from the intercellular to the extracellular space. Using the same logic as we have, Maeno et al. (1977) concluded that the endplate

channel is a pore of 6.4 Å diameter. Their estimate should be smaller than ours because, in taking into account the uncertainty of the moving electrode method, they assumed that those ions giving signals less than 10% of those for Na^+ might not be permeant at all. We should point out that our pore size is also a lower limit, and if we had a better technique capable of measuring permeability ratios in the range 0.001–0.01, new measurements might make it necessary to increase the postulated dimensions. Finally, the pore may not be very rigid and it might be necessary to consider a fluctuating effective size.

ACCESS AND FRICTION Suppose the endplate channel has a water-filled ion-selecting filter of the size represented in Fig. 7, how is the permeability to different ions determined? The correlation with ion size and the lack of correlation with specific chemical properties suggest that a mechanical pore

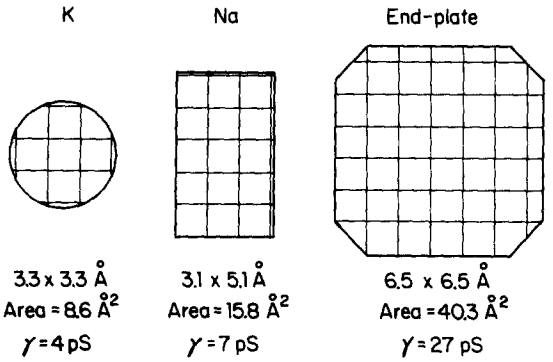

FIGURE 7. Hypothetical cross sections of three types of ionic channels in frog nerve and muscle. The 1-Å grid lines define the area available for diffusion in electrically excitable K channels and Na channels and in the chemically excitable endplate channel. Each minimum pore size was deduced from the dimensions of the permeant and impermeant ions (Hille, 1975; and this paper). The single-channel conductances (γ) were calculated from analysis of stationary current fluctuations (Begenisich and Stevens, 1975; Conti et al., 1976; Neher and Stevens, 1977). The specific conductance of each of these channels is ~0.5 pS/Å^2.

model is needed, such as those used extensively in discussing permeation and filtration of nonelectrolytes in porous biological membranes (Renkin, 1955; Solomon, 1968; Bean, 1972; Verniory et al., 1973; Levitt, 1975). Typically, the pore is idealized as a cylinder with a radius r permeated by spheres of radius a and characterized by the radius ratio α, defined as a/r. Larger molecules enter and move less easily in the pore, because the area available for their diffusion decreases as $(1 - \alpha)^2$ by an excluded volume effect. In addition there may be a drag that increases as a function of a or α. If the pore itself is so short that it offers little friction, the drag might just be aqueous friction, external to the pore and proportional to a. More commonly, the pore walls are considered to create drag, and more complicated hydrodynamic equations for a ball falling through a homogenous viscous medium in a cylinder are applied. In a critique of these theories Bean (1972) has suggested

that there is little point in applying such continuum equations when the pore is almost as small as the water molecules of the medium. As one test of this point, Levitt (1973) made a molecular dynamic simulation of spherical particles moving in a small cylinder and concluded that the classical formulas give too strong a decrease of permeability with particle diameter. Evidently the field needs further development.

Fig. 8 A shows the relative permeability of all the organic monovalent ions studied plotted against molecular diameter, where diameter is defined as the geometric mean of the dimensions of a rectangular box that would contain the ion. Fig. 8 B shows the same permeability values plotted on a logarithmic scale. Three theoretical lines are drawn as well, representing the following

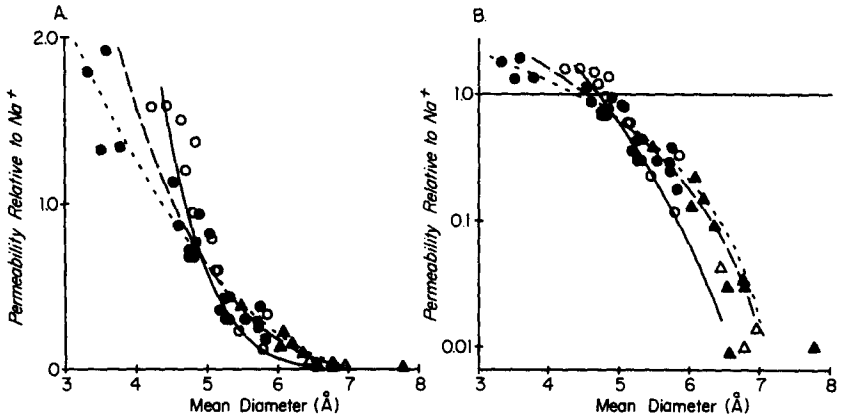

FIGURE 8. Relationship between relative permeability for monovalent organic cations and molecular size. The mean diameters were calculated as the geometric mean of the three dimensions of a space-filling model of the cation, including the effect of hydrogen bonds. The theoretical lines assume a circular pore diameter of 7.4 Å and selectivity based on three possible theories given in text. Short dashes: excluded-volume theory, P_1 (Eq. 3). Long dashes: excluded volume and a drag varying directly as the mean diameter, P_2 (Eq. 4). Solid line: hydrodynamic theory for spheres moving in a cylinder, P_3 (Eq. 5).

three functions which have been scaled arbitrarily to cross at a diameter of 4.9 Å:

$$P_1 = 7 \cdot (1 - \alpha)^2. \tag{3}$$

This function, shown as a dotted line, contains only the relative area correction.

$$P_2 = 17.5 \cdot (1 - \alpha)^2 / a. \tag{4}$$

This function, shown as a dashed line, contains the area factor and a drag proportional to radius (in Å).

$$P_3 = 117 \cdot (1 - \alpha)^2 \cdot \frac{1 - 2.105\alpha + 2.0865\alpha^3 - 1.7068\alpha^5 + 0.72603\alpha^6}{1 - 0.75857\alpha^5}. \tag{5}$$

This function, shown as a solid line, contains the area factor and the drag of a sphere moving through a stationary viscous liquid in a cylinder (Haberman and Sayre, 1958). The power series is the modern equivalent of Faxén's early result (Faxén, 1922) applied by Renkin (1955) and others to porous endothelial cell membranes (see Bean, 1972; Verniory et al., 1973; Levitt, 1975). The pore radius used in evaluating these functions is 3.7 Å (diameter 7.4 Å), a size that gives an area of 43 $Å^2$, similar to that of the square pore drawn in Fig. 7. The predictions of the three theories differ and the vertical scaling is arbitrary. In addition, none of the theories is exactly appropriate to our case. Nevertheless, we suggest from the qualitative similarity of theories and observation that pore size and drag may suffice to explain the major features of relative permeability among organic cations at the endplate channel.

Conclusion

Although in this paper and the next (Adams et al., 1980), we have investigated the permeability to 70 different cations, many other possible test ions remain to be studied. We find that size is a good predictor of permeability to cations and nonelectrolytes. When it is not convenient to measure size, the molecular weight or even the number of major atoms give a fair estimate. The following approximate criteria for permeability may be useful: a substance without negative charges is sure to be permeant if it fits readily through the hole depicted in Fig. 7 or if it weighs less than 135 daltons or has fewer than 10 major atoms. Some substances of larger weight and larger numbers of atoms are permeant provided they fit the hole, e.g., glucosamine or decamethonium. Glucosamine cannot be recommended as the ideal impermeant salt, both because it seems to be measurably permeant and because its pK_a is low enough to make a solution of the chloride salt acid. Arginine and lysine salts are both neutral and less permeant, and are therefore more suitable as inert substitutes. Tetrakisethanolammonium ions are probably impermeant also, but the salts are extremely hygroscopic and the ion blocked endplate currents.

On the basis of the long list of permeant ions, the endplate channel is a larger pore than the Na and K channels of electrically excitable membranes where even methylamine is impermeant (Hille, 1975). The large channel size must contribute to the large single-channel conductance under physiological conditions (Neher and Stevens, 1977) and hence helps to ensure the speed and efficacy of neuromuscular transmission. The large size would also mean that small molecules need not interact closely with the channel walls while passing through, and therefore selectivity among small molecules for size, or even for charge, could be weaker than in Na and K channels. Larger cations fall into a selectivity sequence dominated by frictional factors rather than chemical ones. These questions are considered further in the following paper.

Note Added Since this manuscript was submitted, S. Watanabe and T. Narahashi (1979) have published a paper in which they report permeability ratios for NH_4^+, formamidine, methylamine, and hydrazine agreeing to within 5% of ours.

We thank Lea Miller for invaluable secretarial help and assistance in all phases of this work, Barry Hill for building the electronics, and Dr. Theodore H. Kehl and his staff for providing computer resources. We are grateful to Dr. Wolfgang Nonner and Dr. Wolfhard Almers for reading a draft of the manuscript.

This research was supported by grants NS 08174, NS 05082, and FR 00374 from the National Institutes of Health. Dr. Adams was a Fellow of the Muscular Dystrophy Association of America.

Received for publication 1 November 1979.

REFERENCES

ADAMS, D. J., T. M. DWYER, and B. HILLE. 1980. The permeability of endplate channels to monovalent and divalent metal cations. *J. Gen. Physiol.* **75**:493–510.

BEAN, C. P. 1972. The physics of porous membranes—neutral pores. *In* Membranes, Vol. 1., Macroscopic Systems and Models. G. Eisenman, editor. Marcel Dekker, Inc., New York. 1–54.

BEGENISICH, T., and C. F. STEVENS. 1975. How many conductance states do potassium channels have? *Biophys. J.* **15**:843–846.

CASE, R., R. CREESE, W. J. DIXON, F. J. MASSEY, and D. B. TAYLOR. 1977. Sodium entry in rat diaphragm induced by depolarizing drugs. *J. Physiol. (Lond.).* **272**:283–294.

CONTI, F., B. HILLE, B. NEUMCKE, W. NONNER, and R. STÄMPFLI. 1976. Conductance of the sodium channel in myelinated nerve fibres with modified sodium inactivation. *J. Physiol. (Lond.).* **262**:729–742.

CREESE, R., and J. M. ENGLAND. 1970. Decamethonium in depolarized muscle and the effects of tubocurarine. *J. Physiol. (Lond.).* **210**:345–361.

DWYER, T. M., D. J. ADAMS, and B. HILLE. 1979. Ionic selectivity of end-plate channels. *Biophys. J.* **25**:67a. (Abstr.)

FARLEY, J. M., S. WATANABE, J. Z. YEH, and T. NARAHASHI. 1979. Mechanism of end-plate channel block by N-alkyl guanidine derivatives. *Biophys. J.* **25**:16a. (Abstr.)

FATT, P. 1950. The electromotive action of acetylcholine at the motor end-plate. *J. Physiol. (Lond.).* **111**:408–422.

FATT, P., and B. KATZ. 1951. An analysis of the end-plate potential recorded with an intracellular electrode. *J. Physiol. (Lond.).* **115**:320–370.

FAXÉN, H. 1922. Die Bewegung einer starren Kugel längs der Achse eines mit zäher Flüssigkeit gefüllten Rohres. *Ark. Mat. Astron. Fysik.* **17**:1–28.

FURUKAWA, T., and A. FURUKAWA. 1959. Effects of methyl and ethyl derivative of NH_4^+ on the neuromuscular junction. *Jpn. J. Physiol.* **9**:130–142.

GOLDMAN, D. E. 1943. Potential, impedance and rectification in membranes. *J. Gen. Physiol.* **27**: 37–60.

HABERMAN, W. L., and R. M. SAYRE. 1958. Motion of rigid and fluid spheres in stationary and moving liquids inside cylindrical tubes. David Taylor Model Basin (Dept. of the Navy), Report 1143. U.S. Department of Defense, Navy Department, Washington, D.C.

HILLE, B. 1975. Ionic selectivity of Na and K channels of nerve membranes. *In* Membranes—A Series of Advances, Vol. 3, Dynamic Properties of Lipid Bilayers and Biological Membranes. G. Eisenman, editor. Marcel Dekker, Inc., New York. 255–323.

HILLE, B., and D. T. CAMPBELL. 1976. Am improved Vaseline gap voltage clamp for skeletal muscle fibers. *J. Gen. Physiol.* **67**:265–293.

HODGKIN, A. L., and B. KATZ. 1949. The effect of sodium ions on the electrical activity of the giant axon of the squid. *J. Physiol. (Lond.)*. **108:**37–77.

HOFFMAN, R. 1977. The modulation contrast microscope: principles and performance. *J. Microscopy (Oxf.)* **110** (Pt. 3):205–222.

HUANG, L. M., W. A. CATTERALL, and G. EHRENSTEIN. 1978. Selectivity of cations and nonelectrolytes for acetylcholine-activated channels in cultured muscle cells. *J. Gen. Physiol.* **71:**397–410.

JENKINSON, D. H., and J. G. NICHOLLS. 1961. Contractures and permeability changes produced by acetylcholine in depolarized denervated muscle. *J. Physiol. (Lond.)*. **159:**111–127.

KOKETSU, K., and S. NISHI. 1959. Restoration of neuromuscular transmission in sodium-free hydrazinium solution. *J. Physiol. (Lond.)*. **147:**239–252.

LASSIGNAL, N. L., and A. R. MARTIN. 1977. Effect of acetycholine on postjunctional membrane permeability in eel electroplaque. *J. Gen. Physiol.* **70:**23–36.

LEVITT, D. G. 1973. Kinetics of diffusion and convection in 3.2 Å pores. *Biophys. J.* **13:**186–206.

LEVITT, D. G. 1975. General continuum analysis of transport through pores. I. Proof of Onsager's reciprocity postulate for uniform pore. *Biophys. J.* **15:**533–551.

LEWIS, C. A. 1979. Ion concentration dependence of the reversal potential and the single channel conductance of ion channels at the frog neuromuscular junction. *J. Physiol. (Lond.)*. **286:**417–445.

LINDER, T. M., and D. M. J. QUASTEL. 1978. A voltage-clamp study of the permeability change induced by quanta of transmitter at the mouse endplate. *J. Physiol. (Lond.)*. **281:**535–556.

MAENO, T., C. EDWARDS, and M. ANRAKU. 1977. Permeability of the end-plate membrane activated by acetylcholine to some organic cations. *J. Neurobiol.* **8:**173–184.

NEHER, E., and C. F. STEVENS. 1977. Conductance fluctuations and ionic pores in membranes. *Annu. Rev. Biophys. Bioeng.* **6:**345–381.

OOMURA, Y., and T. TOMITA. 1960. Study on properties of neuromuscular junction. *In* Electrical Activity of Single Cells. Y. Katsuki, editor. Igako Shoin, Ltd., Tokyo. 181–205.

RENKIN, E. M. 1955. Filtration, diffusion, and molecular sieving through porous cellulose membranes. *J. Gen. Physiol.* **38:**225–243.

RITCHIE, A. K., and D. M. FAMBROUGH. 1975. Ionic properties of the acetylcholine receptor in cultured rat myotubes. *J. Gen. Physiol.* **65:**751–767.

SOLOMON, A. K. 1968. Characterization of biological membranes by equivalent pores. *J. Gen. Physiol.* **51** (No. 5, Pt. 2):335s–364s.

TAKEUCHI, N. 1963 *a*. Some properties of conductance changes at the end-plate membrane during the action of acetylcholine. *J. Physiol. (Lond.)*. **167:**128–140.

TAKEUCHI, N. 1963 *b*. Effects of calcium on the conductance change of the end-plate membrane during the action of transmitter. *J. Physiol. (Lond.)*. **167:**141–155.

TAKEUCHI, A., and N. TAKEUCHI. 1960. On the permeability of end-plate membrane during the action of transmitter. *J. Physiol. (Lond.)*. **154:**52–67.

TRAUTMANN, A., and N. F. ZILBER-GACHELIN. 1976. Further investigations on the effect of denervation and pH on the conductance change at the neuromuscular junction of the frog. *Pflügers Arch. Eur. J. Physiol.* **364:**53–58.

VERNIORY, A., R. DU BOIS, P. DECOODT, J. P. GASSEE, and P. P. LAMBERT. 1973. Measurement of the permeability of biological membranes. Application to the glomerular wall. *J. Gen. Physiol.* **62:**489–507.

WATANABE, S., and T. NARAHASHI. 1979. Cation selectivity of acetylcholine-activated ionic channel of frog endplate. *J. Gen. Physiol.* **74:**615–628.